

# Non-abelian Geometric Quantum Energy Pump

Yang Peng<sup>1, 2,\*</sup>

<sup>1</sup>Department of Physics and Astronomy, California State University, Northridge, Northridge, California 91330, USA

<sup>2</sup>Institute of Quantum Information and Matter and Department of Physics,  
California Institute of Technology, Pasadena, CA 91125, USA

We introduce a non-abelian geometric quantum energy pump realized by a transitionless geometric quantum drive—a time-dependent Hamiltonian supplemented by a counterdiabatic term generated by a prescribed trajectory on a smooth control manifold—that coherently transports states within a degenerate subspace. When the coordinates of the trajectory are independently addressable by external drives, the net energy transferred between drives is set by the non-abelian Berry-curvature tensor. The trajectory-averaged pumping power is separately controlled by the initial state and by the Hamiltonian topology through the Euler class. We outline an implementation with artificial atoms, which are realizable on various platforms including trapped atoms/ions, superconducting circuits, and semiconductor quantum dots. The resulting energy pump can serve as a quantum transducer or charger, and as a metrological tool for measuring phase coherences in quantum states.

*Introduction.*— Quantum energy pump, a quantum machine that controls the form and flow of energy among interconnected quantum systems, is one of the most important building block in quantum technology. It can be used as a quantum transducer [1], which converts and transports energy between devices operating at different energy scales [2–4] to create a quantum network [5, 6]. In a different context, the energy pump behaves as a charger [7] that is able to charge a quantum battery [8].

Controllability and sustainability are the two important aspects of an ideal quantum energy pump. Namely, it should be able to process energy of various frequencies at a tunable rate, and for a long enough time. The prior works on topological energy conversion [9–13] have made one big step towards such a pump. However, the topological nature of the pump is reflected on a quantized pumping rate, which limits the tunability. Some of the works [9–11] requires adiabaticity that severely restrict the speed of operation. A more recent work [14] demonstrated an energy conversion can be operated beyond adiabatic regime at a non-quantized rate. However, such rates does not have a simple relation on the system parameters and thus limits its practical usage.

In the field of quantum batteries, the research mainly focuses on finding optimized charging protocols [15, 16], which maximize the energy stored inside the battery in the fastest way. However, the charging in this context is not at a steady rate and final state of the charger is mostly arbitrary. This implies the charger has to be brought to an initial state, which depends on the initial state of an empty battery, after every charging cycle. This violates the requirements that an ideal charger can be operated steadily as long as possible without a reset.

In this Letter, we propose a non-abelian geometric quantum energy pump that addresses the issues of controllability and sustainability. The pump operates in a degenerate subspace under a transitionless geometric quantum drive [Fig. 1 (a)], which keeps system within

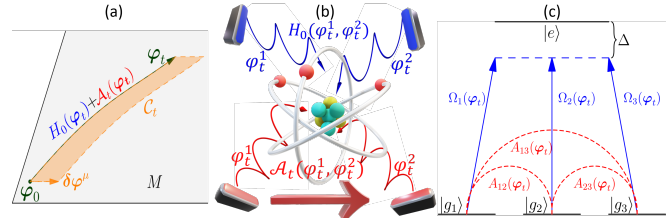


FIG. 1. (a) Transitionless geometric quantum drive: a trajectory (green dashed line)  $\varphi_t$  starting from  $\varphi_0$  on a smooth manifold  $M$ , and a time-dependent Hamiltonian  $H_0(\varphi_t) + \mathcal{A}_t(\varphi_t)$  with  $\mathcal{A}_t$  the Kato gauge potential of  $H_0$ .  $C_t$  is a closed loop in the counterclockwise direction starting at  $\varphi_0$  as indicated by the orange dashed line.  $\delta\varphi^\mu$  is a vector, which is taken to be infinitesimally short, along the  $\mu$ th component of the local coordinate  $\varphi$ . (b) An artificial atom is controlled by  $H_0(\varphi_t) + \mathcal{A}_t(\varphi_t)$ , where we assumed  $\varphi_t = (\varphi_t^1, \varphi_t^2)$ , in which both components can be independently controlled by different protocols, for  $H_0$  and  $\mathcal{A}_t$ , as indicated by blue and red spiral arrows. (c) Tripod system is a concrete realization of the setting in (b).  $H_0$  consists of three degenerate levels  $|g_{1,2,3}\rangle$  which are coupled (blue arrows) to the excited state  $|e\rangle$  at detuning  $\Delta$  with,  $\varphi_t$ -dependent coupling strength  $\Omega_{1,2,3}$ . At large detuning,  $\mathcal{A}_t$  consists couplings between states in the degenerate subspace, as indicated by the red dashed lines.

this subspace along evolution at any speed and for an arbitrary length of time. The non-abelian nature of the evolution within the subspace provides one additional knob that continuously tune the energy pumping rate, simply by changing the initial state of the system. We further demonstrate that such a pump can be realized in an artificial atom with a “tripod” energy levels, as illustrated in Figs. 1 (b,c). Such systems have been realized in labs using trapped atoms/ions [17–20], superconducting circuits [21–26], and semiconductor quantum dots [27–29].

*Transitionless geometric quantum drive.*— Consider a smooth Hamiltonian  $H_0(\varphi)$  defined on a  $d$ -dimensional manifold  $M$ , with local coordinate  $\varphi = (\varphi^1, \varphi^2, \dots, \varphi^d)$ .

Let  $\varphi_t$  be a smooth trajectory on  $M$  parametrized by  $t$  (viewed as time), as illustrated in Fig. 1 (a). The triple  $(H_0, M, \varphi)$  defines a geometric quantum drive [30].

A transitionless geometric quantum drive can be achieved if we evolve an eigenstate of  $H_0(\varphi_0)$  under a new Hamiltonian  $H(\varphi_t) = H_0(\varphi_t) + \mathcal{A}_t(\varphi_t)$ , where  $\mathcal{A}_t$  is the counterdiabatic (CD) term [31–33] that ensures the time-evolved state remains to be an instantaneous eigenstate of  $H_0(\varphi_t)$ . The CD term  $\mathcal{A}_t$  is not unique and one common choice is the Kato gauge potential (KGP) [34–38]  $\mathcal{A}_t = \sum_\mu \dot{\varphi}_t^\mu \mathcal{A}_\mu$ , with

$$\mathcal{A}_\mu(\varphi_t) = \frac{i}{2} \sum_n [\partial_\mu \Pi_{\varphi_t}^n, \Pi_{\varphi_t}^n], \quad (1)$$

where the index  $\mu$  can either be  $t$ , or a directional index  $(1, 2, \dots, d)$  with  $\partial_\mu \equiv \partial/\partial\varphi^\mu$ . We denote the eigenspace projector of the Hamiltonian  $H_0(\varphi)$  at energy  $\epsilon_n(\varphi)$  as  $\Pi_\varphi^n = \sum_\alpha |n\alpha(\varphi)\rangle \langle n\alpha(\varphi)|$ , where  $\{|n\alpha(\varphi)\rangle\}$  are the corresponding (possibly) degenerate (indexed by  $\alpha$ ) eigenstates. Notebly, the KGP is a unique gauge choice that reproduces the phase evolution of eigenstates in an adiabatic evolution exactly. The instantaneous eigenstates are parallel transported along the trajectory  $\varphi_t$  according to [38]

$$|n\alpha(\varphi_t)\rangle = \mathcal{W}(\varphi_t \leftarrow \varphi_0) |n\alpha(\varphi_0)\rangle, \quad (2)$$

where  $\mathcal{W}(\varphi_t \leftarrow \varphi_0) = \mathcal{T} \exp(-i \int_0^t dt' \mathcal{A}_t(\varphi_{t'}))$  is the Wilson line operator ( $\mathcal{T}$  refers to as the time ordering operator).

*Energy pumping.*— Let us view  $H_0(\varphi)$  as an intrinsic time-dependent system, such as a driven artificial atom, as depicted in Fig. 1 (b). Further, we add additional drives (viewed as battery or other devices connected to the pump) to create the KGP  $\mathcal{A}_t(\varphi_t)$ , in which each component  $\varphi_t^\mu$  can be controlled independently by the  $\mu$ th driving protocol. We initialize the system in an eigenstate of a degenerate subspace of  $H_0(\varphi_0)$ , namely choosing the initial state  $|\psi(0)\rangle = \Pi_{\varphi_0}^n |\psi(0)\rangle$ . We consider the energy (integrated power) pumped [9–14] into the  $\mu$ th drive (of the KGP)

$$E_\mu(\varphi_t) = \int_0^t ds \dot{\varphi}_s^\mu \langle \psi(s) | \partial_\mu \mathcal{A}_t(\varphi_s) | \psi(s) \rangle \quad (3)$$

where  $|\psi(s)\rangle$  is the time evolved state at time  $s$  under  $H(\varphi_t)$ .

Since the driving is transitionless, we have

$$|\psi(t)\rangle = e^{-i \int_0^t ds \epsilon_n(\varphi_s)} \mathcal{W}(\varphi_t \leftarrow \varphi_0) |\psi(0)\rangle, \quad (4)$$

which enables us to obtain  $E_\mu(\varphi_t) = \int_0^t ds \dot{\varphi}_s^\mu F_{t\mu}^\psi(\varphi_s)$ , where  $F_{t\mu}^\psi(\varphi_t) = \langle \psi(t) | \mathcal{F}_{t\mu}^n(\varphi_t) | \psi(t) \rangle$  is the expectation value of the non-abelian Berry curvature tensor [38, 39] on the  $n$ th eigensubspace, which is defined as

$$\mathcal{F}_{\mu\nu}^n(\varphi_t) = i[\partial_\mu \Pi_{\varphi_t}^n, \partial_\nu \Pi_{\varphi_t}^n]. \quad (5)$$

With an initial basis set  $\{|n\alpha(\varphi_0)\rangle\}$ , one can parametrize  $|\psi(0)\rangle = \sum_\alpha c_\alpha |n\alpha(\varphi_0)\rangle$ , then the pumped energy can also be written as [38]

$$E_\mu(\varphi_t) = \sum_{\nu \neq \mu} \sum_{\alpha\beta} c_\alpha^* c_\beta \int_0^t ds \dot{\varphi}_s^\nu \dot{\varphi}_s^\mu F_{\nu\mu}^{\alpha\beta}(\varphi_s), \quad (6)$$

where only index  $\nu$  is summed, and  $F_{\nu\mu}^{\alpha\beta} = \langle n\alpha | \mathcal{F}_{\nu\mu}^n | n\beta \rangle$ .

For simplicity, we shall choose  $M$  to be an orientable closed manifold, say a  $d$ -torus  $\mathbb{T}^d$ , and parametrize

$$\varphi_t^i = \varphi_0^i + f^i(t) \quad (7)$$

with identification of  $\varphi_t^i = \varphi_{t+2\pi}^i$ . Here, we assume that the function  $f^i(t)$ 's time derivative,  $\dot{f}^i(t)$ , has a slow time dependence can be regarded as the driving frequencies that can be adjusted in time.

Note that the driving trajectory  $\varphi^t$  depends on the initial driving phases  $\varphi_0^i$ , which are initial position of the trajectory on the manifold and are presumably undetermined in experiments. Hence, a more interesting physical quantity should be  $\bar{E}_\mu(t)$  which is the pumped energy up to time  $t$  averaged over initial phases. This can be done if one either perform experiment on a single artificial many times, or consider an ensemble of many artificial atoms which have random initial phases. This average is calculated by performing an integration on the manifold, which is  $\bar{E}_\mu(t) = \sum_{\nu \neq \mu} \int_0^t ds \bar{P}_{\nu\mu}(s)$ , where we introduced instantaneous pumping power (averaged over initial phases) from drive  $\nu$  to drive  $\mu$  as

$$\bar{P}_{\nu\mu}(t) = \sum_{\alpha\beta} c_\alpha^* c_\beta F_{\nu\mu}^{\alpha\beta} \dot{f}^\nu(t) \dot{f}^\mu(t). \quad (8)$$

Here, we have introduced the averaged non-abelian Berry curvature  $\bar{F}_{\mu\nu}^{\alpha\beta} = \int d\varphi^\mu d\varphi^\nu F_{\mu\nu}^{\alpha\beta}/(4\pi^2)$ , where the integration is on the submanifold of  $(\varphi^\mu, \varphi^\nu)$ .

Before introducing experimental realization, we comment on the reason why we choose the KGP  $\mathcal{A}_t(\varphi_t)$ , not the entire  $H(\varphi_t)$  as driving term for the energy pump. This is because the term  $H_0(\varphi_t)$ , which is the other contribution in  $H(\varphi_t)$ , does not produce any pumping power when phase average is conducted. To see this, we can write down the energy pumped due to  $H_0$  as

$$E'_\mu(\varphi_t) = \int_0^t ds \dot{\varphi}_s^\mu \langle \psi(s) | \partial_\mu H_0(\varphi_s) | \psi(s) \rangle. \quad (9)$$

Since  $|\psi(s)\rangle$  is an instantaneous eigenstate, we can apply the Hellmann–Feynman theorem, and write the integrand as  $\dot{\varphi}_s^\mu \partial_\mu \epsilon_n(\varphi_s)$ . This term averages to zero over random initial phases if one takes the parametrization in Eq. (7).

*Experimental Realization.*—A convenient physical implementation uses three long-lived states  $|g_i\rangle$  ( $i = 1, 2, 3$ ) coupled to a common excited state  $|e\rangle$  (“tripod” system) with a common one-photon detuning  $\Delta$  and

time-dependent Rabi rates  $\Omega_i(t) \in \mathbb{R}$  for each state  $|g_i\rangle$ , which can be controlled independently. This is described by the following time-dependent Hamiltonian  $H_0(\varphi_t) = \Delta|e\rangle\langle e| + V(\varphi_t) + V^\dagger(\varphi_t)$ , where  $V(\varphi) = \sum_{i=1}^3 \Omega_i(\varphi)|e\rangle\langle g_i|$ . Such a setup can be realized experimentally in various physical platforms [17–29].

This Hamiltonian has a doubly degenerate dark state subspace at zero energy, denoted as  $\ker H_0$ , which is orthogonal to the excited state  $|e\rangle$  and the superposition state  $|\tilde{g}\rangle = \sum_j \Omega_j |g_j\rangle / \Omega$ , where  $\Omega = \sqrt{\sum_i \Omega_i^2}$ .  $H_0$  also admits two non-degenerate states  $|\psi_\pm\rangle$  at finite energies  $\epsilon_\pm = (\Delta \pm \sqrt{\Delta^2 + 4\Omega^2})/2$ . These two finite energy eigenstates are obtained by superpositions of  $|e\rangle$  and  $|\tilde{g}\rangle$ .

Let us initialize the system in a dark state  $|\psi(0)\rangle \in \ker H_0(\varphi_0)$ , which can be done using the technique coherent population transfer [40, 41]. To ensure the time-evolving state  $|\psi(t)\rangle$  stays within the dark state subspace, we need to add the counter-diabatic (CD) term, i.e. the KGP introduced previously. Actually, we only need to construct the KGP projected onto the subspace spanned by the three long-lived states  $\{|g_i\rangle\}$ . To see this, assuming  $|\psi(t)\rangle \in \ker H_0(\varphi_t)$ , then consider infinitesimal evolution

$$|\psi(t+dt)\rangle = |\psi(t)\rangle - idtH(\varphi_t)|\psi(t)\rangle = |\psi(t)\rangle, \quad (10)$$

which is orthogonal to  $|e\rangle$ . Thus, in order to maintain  $|\psi(t+dt)\rangle \in \ker H_0(\varphi_{t+dt})$ , we just need to ensure  $\langle\psi(t+dt)|\tilde{g}(t+dt)\rangle = 0$ , which can be done by adding the subspace projected KGP mentioned above. By induction,  $|\psi(t)\rangle$  stays to be a dark state.

Let us denote eigenstate projector  $\Pi_{\varphi_t} = |\tilde{g}(\varphi_t)\rangle\langle\tilde{g}(\varphi_t)|$ , the projected KGP can be computed as  $\mathcal{A}_t = i[\Pi_{\varphi_t}, \Pi_{\varphi_t}]$ . By straightforward calculation, we can explicitly write it as  $\mathcal{A}_t = i \sum_{jk} A_{jk} |g_j\rangle\langle g_k|$ , where [38]

$$A_{jk}(\varphi_t) = \frac{1}{\Omega(\varphi_t)^2} (\dot{\Omega}_j(\varphi_t)\Omega_k(\varphi_t) - \dot{\Omega}_k(\varphi_t)\Omega_j(\varphi_t)). \quad (11)$$

These terms can be implemented with the two-photon Raman processes [42, 43] which has been realized experimentally [24–26].

Since the Hamiltonian  $H_0$  is real symmetric, we can choose two 3D real vectors  $\mathbf{u}_1 \equiv |u_1\rangle$ , and  $\mathbf{u}_2 \equiv |u_2\rangle$  as the two instantaneous basis states of  $\ker H_0$ , at each  $\varphi$ , such that  $|\tilde{g}\rangle \equiv \tilde{\mathbf{g}} = \mathbf{u}_1 \times \mathbf{u}_2$ , where  $\times$  denotes the cross product of vectors in  $\mathbb{R}^3$ . The non-abelian Berry curvature in basis  $|u_1\rangle, |u_2\rangle$  has zero diagonal components, due to reality of the states. It can have nonzero off-diagonal elements  $F_{\nu\mu}^{12} = -F_{\nu\mu}^{12}$ , also known as the Euler form [44, 45], which is given by

$$\text{Eu}_{\nu\mu} \equiv -iF_{\nu\mu}^{12} = \tilde{\mathbf{g}} \cdot (\partial_\nu \tilde{\mathbf{g}} \times \partial_\mu \tilde{\mathbf{g}}) \quad (12a)$$

$$= \langle \partial_\nu u_1 | \partial_\mu u_2 \rangle - i \langle \partial_\nu u_2 | \partial_\mu u_1 \rangle. \quad (12b)$$

Writing  $|\psi(t)\rangle = c_1 |u_1(\varphi_t)\rangle + c_2 |u_2(\varphi_t)\rangle$ , and plug it into Eq. (6), we have

$$E_\mu(\varphi_t) = -2\text{Im}(c_1^* c_2) \sum_{\nu \neq \mu} \int_0^t ds \dot{\varphi}_s^\nu \dot{\varphi}_s^\mu \text{Eu}_{\nu\mu}(\varphi_s). \quad (13)$$

Let us take the parametrization in Eq. (7), and write  $c_1 = ce^{i\phi_1}$ ,  $c_2 = \sqrt{1-c^2}e^{i\phi_2}$ . If we perform average over initial drive phases, we obtain the instantaneous pumping power from drive  $\nu$  to drive  $\mu$  defined in Eq. (8) as

$$\bar{P}_{\nu\mu}(t) = \dot{f}^\nu(t) \dot{f}^\mu(t) c \sqrt{1-c^2} \sin(\delta\phi) \frac{\chi_{\nu\mu}}{\pi} \quad (14)$$

where  $\delta\phi = \phi_1 - \phi_2$ . Here, averaging  $\text{Eu}_{\nu\mu}$  gives the Euler class on the corresponding submanifold, defined as [44, 45]

$$\chi_{\nu\mu} = \int d\varphi^\nu d\varphi^\mu \text{Eu}_{\nu\mu} / (2\pi) \quad (15)$$

which is always an even integer. Eq. (14) is the central result of this letter, which demonstrates a high controllability of the instantaneous pumping power on this non-abelian quantum energy pump. The power is maximized (in absolute value) at  $c = 1/2$  and  $\delta\phi = \pm\pi/2$ , in which flipping the sign of  $\delta\phi$  corresponds to reversing the pumping direction. Since the phase coherence information appears in the pumping power as  $\sin\delta\phi$ , we can also interpret the non-abelian energy pumping as a quantum interference phenomena.

*Two-tone drive example.*— As an illustration, we fix the manifold  $M = \mathbb{T}^2$ , with two coordinates  $\varphi_t = (\varphi_1^1, \varphi_1^2)$ , with parametrization  $\varphi_t^i = \varphi_0^i + \omega_i t$ . We then choose  $\Omega_1(\varphi_t) = m - \cos(\varphi_t^1) - \cos(\varphi_t^2)$ ,  $\Omega_2(\varphi_t) = \sin \varphi_t^1$ ,  $\Omega_3(\varphi_t) = \sin \varphi_t^2$ . This gives nontrivial Euler class  $\chi_{21} = -\chi_{12} = \pm 2$ , when  $m$  is between 0 and  $\pm 2$ .

When  $\omega_1/\omega_2$  is a irrational number, the time-dependence becomes quasiperiodic, whereas if  $\omega_1/\omega_2 = q/p$ , with integers  $p, q$ , the system is time-periodic. Experimentally, the ratio of the two frequencies is always a rational number and we thus write  $\omega_1 = \omega$ , and  $\omega_2 = (p/q)\omega$  in the following. The quasiperiodic case can be obtained as we can approximate any irrational number as a integer ratio. For example, the golden ratio  $\frac{\sqrt{5}+1}{2} \simeq \frac{F_{N+1}}{F_N}$  where  $F_N$  is the  $N$ th Fibonacci number [46]. This approximation gets better as  $N$  increases.

To test our analytical result in Eq. (14), we numerically evolve an initial state prepared in the ground state manifold of  $H_0(\varphi_0)$ , with a random chosen initial phases  $(\varphi_0^1, \varphi_0^2)$ , and compute the pumped energy for drive 2,  $E_2(\varphi_t) = -E_1(\varphi_t)$ , according to Eq. (3). In Fig. 2 (a), we show  $E_2(\varphi_t)$  in colors, for five different trajectories initialized at random phases for parameters  $m = 1, c = 1/\sqrt{2}, \delta\phi = \pi/2, p/q = 3/2$ . We see that the magnitude of pumped energy overall grows linearly in time. On top of that, small oscillations are also visible. Since  $p/q$  is

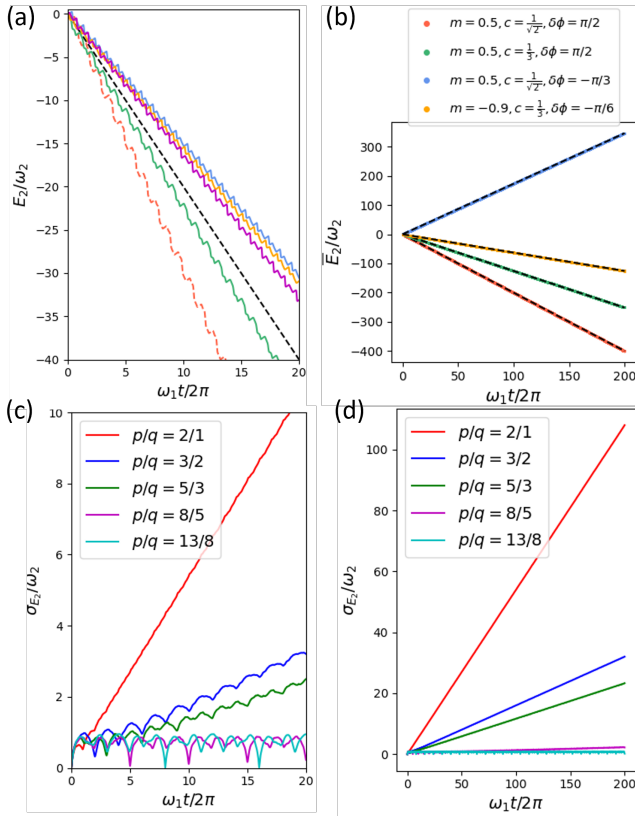


FIG. 2. (a) Pumped energy  $E_2(\varphi_t)$  into drive 2 of the two-tone drive example. Five trajectories at different random initial phases are shown in colors. The black dashed line is phase-averaged result based on Eq. (14). The parameters used are  $m = 0.5, c = 1/\sqrt{2}, \delta\phi = \pi/2, p/q = 3/2$ . (b) Pumped energy  $\bar{E}_2(t)$  into drive 2 averaged over 400 random initial phases sampled uniformly from 0 to  $2\pi$ . The ratio is fixed at  $p/q = 3/2$ . The different sets of other parameters that control the energy pumping power are indicated in different color. The black dashed line is the analytically result. (c,d) Standard deviation  $\sigma_{E_2}$  of  $E_2$  at different  $p/q$  ratios for the 400 trajectories from different initializations, plotted with different time scale. We fix  $c = 1/\sqrt{2}, \delta\phi = \pi/2, m = 0.5$ . The common parameters in all figures are  $\omega = 0.4, \Delta = 1$ .

far away from a irrational number, the slope of the linear trends deviates from the one for the phase-averaged rate  $\bar{E}_2(t)/\omega_2 = -\omega_1 t/\pi$ , indicated by the black lines.

In Fig. 2 (b), we show the pumped energy  $\bar{E}_2(t)$  at different set of parameters, averaged over 400 trajectories at different random initial phases uniformly sampled between 0 and  $2\pi$ . We see a robust energy pumping at steady rates, coincide with the depicted in black dashed lines, obtained from the phase-averaged pumping power calculated analytically in Eq. (14). Notably, the direction and magnitude of the pumping power can be controlled by either tuning the Hamiltonian parameter  $m$ , or choosing the initial state parameters  $c$  and  $\delta\phi$ .

To quantify how does the pumped energy deviate from its phase-averaged value, we introduce the standard

deviation of  $E_2$ ,

$$\sigma_{E_2}(t) = \sqrt{\sum_{i=1}^N \frac{(E_2(\varphi_t^{(i)}) - \bar{E}_2(t))^2}{N}}, \quad (16)$$

where we consider  $N$  trajectories  $\{\varphi_t^{(i)}\}$  indexed by  $i$  that give different pumped energy  $E_2(\varphi_t^{(i)})$ . In Figs. 2 (c,d), we show the results at different time scale with  $N = 400$  at different  $p/q$  ratios, generated by ratios of neighboring Fibonacci numbers. We find that  $\sigma_{E_2}$  overall increases linearly in time, with additional small oscillations. The slope of this linear trend, due to Eq. (13), is proportional to the difference between the Euler form averaged over subregion explored by individual trajectory  $\varphi_t^{(i)}$ , and the one averaged over the entire manifold (which gives the Euler class  $\chi$ ). Note that for rational  $p/q$ , the trajectory always form a closed orbit on  $\mathbb{T}^2$ . When  $p, q$  are large integers, the trajectory is a huge orbit of length  $\sim 2\pi q$  wrapping around the  $\mathbb{T}^2$ , and thus explore most of the region of the manifold. Hence, the deviation from the trajectory-averaged value decays as the ratio  $p/q$  approaches the quasiperiodic limit.

*Conclusions and outlook.*— In this work, we introduced the non-abelian geometric quantum energy pump, by exploiting a transitionless geometric quantum drive that evolves a quantum state within its degenerate subspace. The pump provides a steady, persistent and highly tunable pumping power, which satisfies the criteria being an ideal pump. We showed that the pumping power has a quantum geometric meaning as it is related to the non-abelian Berry curvature tensor. We proposed experimental realization of such a pump based on an artificial atom controlled by multiple independent driving fields, which has already been realized in various physical systems like trapped atoms/ions, superconducting circuits, and semiconductor quantum dots.

We used a two-tone drive example to compute the pumped energy into one of the drive explicitly, and demonstrated both analytically and numerically that the pumping power is controlled independently by the initial state property, and the Euler class, the topological property, of the system Hamiltonian  $H_0$ .

The quantum energy pump we proposed is potentially useful in quantum technology, as a quantum transducer or a quantum charger. Alternatively, since the pumping power is sensitive to the phase coherence property of the initial state inside the degenerate manifold, the quantum energy pump setup could be also used to extract phase coherence information of a quantum state. These practical applications require connecting the quantum energy pump to external devices, such as cavities, qubits etc., which requires explicit modeling and is beyond the scope of this work. We shall explore these directions in future.

*Acknowledgment.*— This work is supported by the US National Science Foundation (NSF) Grant No. PHY-2216774. The numerical simulation is supported by NSF instrument grant DMR-2406524.

\* yang.peng@csun.edu

[1] N. Lauk, N. Sinclair, S. Barzanjeh, J. P. Covey, M. Saffman, M. Spiropulu, and C. Simon, Perspectives on quantum transduction, *Quantum Science and Technology* **5**, 020501 (2020).

[2] C. D. Bruzewicz, J. Chiaverini, R. McConnell, and J. M. Sage, Trapped-ion quantum computing: Progress and challenges, *Applied physics reviews* **6** (2019).

[3] M. Kjaergaard, M. E. Schwartz, J. Braumüller, P. Krantz, J. I.-J. Wang, S. Gustavsson, and W. D. Oliver, Superconducting qubits: Current state of play, *Annual Review of Condensed Matter Physics* **11**, 369 (2020).

[4] G. Burkard, T. D. Ladd, A. Pan, J. M. Nichol, and J. R. Petta, Semiconductor spin qubits, *Rev. Mod. Phys.* **95**, 025003 (2023).

[5] H. J. Kimble, The quantum internet, *Nature* **453**, 1023 (2008).

[6] M. Caleffi, L. d’Avossa, X. Han, and A. S. Cacciapuoti, Quantum transduction: Enabling quantum networking, arXiv preprint arXiv:2505.02057 (2025).

[7] H. Schmid, F. von Oppen, G. Refael, and Y. Peng, to appear (2025).

[8] F. Campaioli, S. Gherardini, J. Q. Quach, M. Polini, and G. M. Andolina, Colloquium: Quantum batteries, *Rev. Mod. Phys.* **96**, 031001 (2024).

[9] I. Martin, G. Refael, and B. Halperin, Topological frequency conversion in strongly driven quantum systems, *Phys. Rev. X* **7**, 041008 (2017).

[10] Y. Peng and G. Refael, Topological energy conversion through the bulk or the boundary of driven systems, *Phys. Rev. B* **97**, 134303 (2018).

[11] F. Nathan, I. Martin, and G. Refael, Topological frequency conversion in a driven dissipative quantum cavity, *Phys. Rev. B* **99**, 094311 (2019).

[12] P. J. D. Crowley, I. Martin, and A. Chandran, Half-integer quantized topological response in quasiperiodically driven quantum systems, *Phys. Rev. Lett.* **125**, 100601 (2020).

[13] Z. Qi, G. Refael, and Y. Peng, Universal nonadiabatic energy pumping in a quasiperiodically driven extended system, *Phys. Rev. B* **104**, 224301 (2021).

[14] C. Psaroudaki and G. Refael, Energy transfer in random-matrix ensembles of floquet hamiltonians, *Phys. Rev. B* **108**, 064301 (2023).

[15] F. Mazzoncini, V. Cavina, G. M. Andolina, P. A. Erdman, and V. Giovannetti, Optimal control methods for quantum batteries, *Phys. Rev. A* **107**, 032218 (2023).

[16] R. Rodriguez, B. Ahmadi, G. Suárez, P. Mazurek, S. Barzanjeh, and P. Horodecki, Optimal quantum control of charging quantum batteries, *New Journal of Physics* **26**, 043004 (2024).

[17] Y. Han, J. Xiao, Y. Liu, C. Zhang, H. Wang, M. Xiao, and K. Peng, Interacting dark states with enhanced nonlinearity in an ideal four-level tripod atomic system, *Phys. Rev. A* **77**, 023824 (2008).

[18] G. Juzeliūnas, J. Ruseckas, A. Jacob, L. Santos, and P. Öhberg, Double and negative reflection of cold atoms in non-abelian gauge potentials, *Phys. Rev. Lett.* **100**, 200405 (2008).

[19] L. Feng, W. L. Tan, A. De, A. Menon, A. Chu, G. Pagano, and C. Monroe, Efficient ground-state cooling of large trapped-ion chains with an electromagnetically-induced-transparency tripod scheme, *Phys. Rev. Lett.* **125**, 053001 (2020).

[20] W. Zhao, Y.-B. Yang, Y. Jiang, Z. Mao, W. Guo, L. Qiu, G. Wang, L. Yao, L. He, Z. Zhou, *et al.*, Quantum simulation for topological euler insulators, *Communications Physics* **5**, 223 (2022).

[21] L. Faoro, J. Siewert, and R. Fazio, Non-abelian holonomies, charge pumping, and quantum computation with josephson junctions, *Phys. Rev. Lett.* **90**, 028301 (2003).

[22] I. Kamleitner, P. Solinas, C. Müller, A. Shnirman, and M. Möttönen, Geometric quantum gates with superconducting qubits, *Phys. Rev. B* **83**, 214518 (2011).

[23] A. A. Abdumalikov Jr, J. M. Fink, K. Juliusson, M. Pechal, S. Berger, A. Wallraff, and S. Filipp, Experimental realization of non-abelian non-adiabatic geometric gates, *Nature* **496**, 482 (2013).

[24] S. Kumar and et al., Stimulated raman adiabatic passage in a three-level superconducting circuit, *Nat. Commun.* **7**, 10628 (2016).

[25] A. Vepsäläinen, S. Danilin, and G. S. Paraoanu, Superadiabatic population transfer in a three-level superconducting circuit, *Science Advances* **5**, eaau5999 (2019).

[26] S. Dogra, A. Vepsäläinen, and G. S. Paraoanu, Experimental demonstration of robustness under scaling errors for superadiabatic population transfer in a superconducting circuit, *Phil. Trans. R. Soc. A* **380**, 20210274 (2022).

[27] J. Houel, J. H. Prechtel, A. V. Kuhlmann, D. Brunner, C. E. Kuklewicz, B. D. Gerardot, N. G. Stoltz, P. M. Petroff, and R. J. Warburton, High resolution coherent population trapping on a single hole spin in a semiconductor quantum dot, *Phys. Rev. Lett.* **112**, 107401 (2014).

[28] S. G. Carter, S. C. Badescu, A. S. Bracker, M. K. Yakes, K. X. Tran, J. Q. Grim, and D. Gammon, Coherent population trapping combined with cycling transitions for quantum dot hole spins using triplet trion states, *Phys. Rev. Lett.* **126**, 107401 (2021).

[29] Y. Zhou, J. Leng, K. Wang, F. Gao, G. Xu, H. Liu, R.-L. Ma, G. Cao, J. Zhang, G.-C. Guo, *et al.*, Quantum interference and coherent population trapping in a double quantum dot, *Nano Letters* **24**, 10040 (2024).

[30] J. Wu, C. Liu, D. Bulmash, and W. W. Ho, Geometric quantum drives: Hyperbolically driven quantum systems and beyond, arXiv preprint arXiv:2503.08242 10.48550/arXiv.2503.08242 (2025).

[31] M. Demirplak and S. A. Rice, Adiabatic population transfer with control fields, *J. Phys. Chem. A* **107**, 9937 (2003).

[32] M. Demirplak and S. A. Rice, On the consistency, extremal, and global properties of counterdiabatic fields, *J. Chem. Phys.* **129** (2008).

[33] M. V. Berry, Transitionless quantum driving, *Journal*

of Physics A: Mathematical and Theoretical **42**, 365303 (2009).

[34] T. Kato, On the adiabatic theorem of quantum mechanics, *Journal of the Physical Society of Japan* **5**, 435 (1950).

[35] J. C. Budich and B. Trauzettel, From the adiabatic theorem of quantum mechanics to topological states of matter, *physica status solidi (RRL)–Rapid Research Letters* **7**, 109 (2013).

[36] P. M. Schindler and M. Bükov, Geometric floquet theory, *Phys. Rev. X* **15**, 031037 (2025).

[37] C. W. Duncan, P. M. Poggi, M. Bükov, N. T. Zinner, and S. Campbell, Taming quantum systems: A tutorial for using shortcuts-to-adiabaticity, quantum optimal control, and reinforcement learning, *PRX Quantum* **6**, 040201 (2025).

[38] See Supplemental Material (SM) for additional details on the KGP, the derivation of the energy pumping formula, and explicit computation of the KGP in the tripod system..

[39] F. Wilczek and A. Zee, Appearance of gauge structure in simple dynamical systems, *Phys. Rev. Lett.* **52**, 2111 (1984).

[40] K. Bergmann, H. Theuer, and B. W. Shore, Coherent population transfer among quantum states of atoms and molecules, *Rev. Mod. Phys.* **70**, 1003 (1998).

[41] N. V. Vitanov, A. A. Rangelov, B. W. Shore, and K. Bergmann, Stimulated raman adiabatic passage in physics, chemistry, and beyond, *Rev. Mod. Phys.* **89**, 015006 (2017).

[42] X. Chen, I. Lizuain, A. Ruschhaupt, D. Guéry-Odelin, and J. G. Muga, Shortcut to adiabatic passage in two- and three-level atoms, *Phys. Rev. Lett.* **105**, 123003 (2010).

[43] J. Dalibard, F. Gerbier, G. Juzeliūnas, and P. Öhberg, Colloquium: Artificial gauge potentials for neutral atoms, *Rev. Mod. Phys.* **83**, 1523 (2011).

[44] F. N. Ünal, A. Bouhon, and R.-J. Slager, Topological euler class as a dynamical observable in optical lattices, *Phys. Rev. Lett.* **125**, 053601 (2020).

[45] A. Bouhon, Q. Wu, R.-J. Slager, H. Weng, O. V. Yazyev, and T. Bzdusek, Non-abelian reciprocal braiding of weyl points and its manifestation in zrte, *Nature Physics* **16**, 1137 (2020).

[46] H. Schmid, Y. Peng, G. Refael, and F. von Oppen, Self-similar phase diagram of the fibonacci-driven quantum ising model, *Phys. Rev. Lett.* **134**, 240404 (2025).

## SUPPLEMENTAL MATERIAL

### PROPERTIES OF KATO GAUGE POTENTIAL (KGP)

Consider a smooth Hamiltonian  $H_0(\varphi)$  with parameters  $\varphi = (\varphi^1, \varphi^2, \dots)$  defined on a smooth manifold  $M$ . Let us denote the eigenspace projector as  $\Pi_{\varphi}^n$ . In the following, we provide several theorems that describe the properties of the KGP.

**Theorem 1.** *Define the KGP along the direction  $\varphi_\mu$  as*

$$\mathcal{A}_\mu(\varphi) = \frac{i}{2} \sum_n [\partial_\mu \Pi_{\varphi}^n, \Pi_{\varphi}^n] \quad (17)$$

where  $\partial_\mu \equiv \partial/\partial\varphi^\mu$ . We have

$$\Pi_{\varphi}^n \mathcal{A}_\mu(\varphi) \Pi_{\varphi}^n = 0 \quad (18)$$

Consider a smooth curve on  $M$  denoted as  $\varphi_t$  parameterized by  $t$  (viewed as time). Let us initialize the system in an eigenstate  $|\psi(0)\rangle \equiv \Pi_{\varphi_0}^n |\psi(0)\rangle$  of  $H(\varphi_{t=0})$ .

**Theorem 2.** *Let us construct the time-dependent Hamiltonian  $H(\varphi_t) = H_0(\varphi_t) + \mathcal{A}_t(\varphi_t)$ , and consider the Schrödinger equation*

$$i\partial_t |\psi(t)\rangle = H(\varphi_t) |\psi(t)\rangle, \quad (19)$$

under the initial condition  $|\psi(0)\rangle = \Pi_{\varphi_0}^n |\psi(0)\rangle$ , then  $\Pi_{\varphi_t}^n |\psi(t)\rangle = |\psi(t)\rangle$  at any time  $t$ . Thus,  $\mathcal{A}_t$  is the counterdiabatic term.

*Proof.* We can consider an infinitesimal  $\delta t \rightarrow 0$  time evolution (neglecting terms  $o(\delta t^2)$ )

$$|\psi(t + \delta t)\rangle = |\psi(t)\rangle - i\delta t [H_0(\varphi_t) + \mathcal{A}_t(\varphi_t)] |\psi(t)\rangle, \quad (20)$$

and compute

$$\Pi_{\varphi_{t+\delta t}}^n |\psi(t + \delta t)\rangle = \left[ \Pi_{\varphi_t}^n + \delta t \partial_t \Pi_{\varphi_t}^n \right] [1 - i\delta t H_0(\varphi_t) - i\delta t \mathcal{A}_t(\varphi_t)] |\psi(t)\rangle \quad (21)$$

$$= \left[ \Pi_{\varphi_t}^n - \delta t \left( i \Pi_{\varphi_t}^n H_0(\varphi_t) + i \Pi_{\varphi_t}^n \mathcal{A}_t(\varphi_t) - \partial_t \Pi_{\varphi_t}^n \right) \right] |\psi(t)\rangle. \quad (22)$$

Note that  $[H_0(\varphi_t), \Pi_{\varphi_t}^n] = 0$  and  $\mathcal{A}_t(\varphi_t)$  has no matrix elements between states at the same energy, namely  $\Pi_{\varphi_t}^n \mathcal{A}_t(\varphi_t) \Pi_{\varphi_t}^n = 0$ , by Theorem 1. Assuming  $\Pi_{\varphi_t}^n |\psi(t)\rangle = |\psi(t)\rangle$ , we have

$$\mathcal{A}_t(\varphi_t) |\psi(t)\rangle = i(\partial_t \Pi_{\varphi_t}^n) |\psi(t)\rangle.$$

and thus

$$\Pi_{\varphi_{t+\delta t}}^n |\psi(t + \delta t)\rangle = [1 - i\delta t (H_0(\varphi_t) + \mathcal{A}_t(\varphi_t))] |\psi(t)\rangle = |\psi(t + \delta t)\rangle. \quad (23)$$

Hence,  $\Pi_{\varphi_t}^n |\psi(t)\rangle = |\psi(t)\rangle$  whenever  $\Pi_{\varphi_0}^n |\psi(0)\rangle = |\psi(0)\rangle$ .  $\square$

Because of Theorem 2, if one takes  $\{|n\alpha\rangle\}$  as a basis for the eigensubspace of  $H_0(\varphi_0)$  at energy  $\epsilon_n(\varphi_0)$ , we can define a parallelly transported basis along the trajectory  $\varphi_t$  as  $\{|n\alpha(\varphi_t)\rangle\}$ , with  $|n\alpha(\varphi_0)\rangle \equiv |n\alpha\rangle$ . Explicitly, we can write

$$|n\alpha(\varphi_t)\rangle = \mathcal{W}(\varphi_t \leftarrow \varphi_0) |n\alpha(\varphi_0)\rangle, \quad (24)$$

with Wilson line operator generated by the KGP  $\mathcal{A}_t$

$$\mathcal{W}(\varphi_t \leftarrow \varphi_0) = \mathcal{T} \exp(-i \int_0^t dt' \mathcal{A}_t(\varphi_{t'})) = \mathcal{P} \exp(-i \int_{\varphi_t} d\varphi \cdot \mathcal{A}(\varphi)), \quad (25)$$

where  $\mathcal{A} = (\mathcal{A}_1, \mathcal{A}_2, \dots, \mathcal{A}_d)$ . This means that from an initial state  $|\psi(0)\rangle$  in this subspace, parametrized as

$$|\psi(0)\rangle = \sum_{\alpha} c_{\alpha} |n\alpha(\varphi_0)\rangle, \quad (26)$$

the time-evolved state can be written as

$$|\psi(t)\rangle = e^{-i \int_0^t ds \epsilon_n(\varphi_s)} \mathcal{W}(\varphi_t \leftarrow \varphi_0) = e^{-i \int_0^t ds \epsilon_n(\varphi_s)} \sum_{\alpha} c_{\alpha} |n\alpha(\varphi_t)\rangle. \quad (27)$$

This implies that the expectation value of any operator  $\mathcal{F}$ , the expectation value can be computed as

$$\langle \psi(s) | \mathcal{F} | \psi(s) \rangle = \sum_{\alpha\beta} c_{\alpha}^* c_{\beta} F^{\alpha\beta}, \quad F^{\alpha\beta} = \langle \alpha | \mathcal{F} | \beta \rangle. \quad (28)$$

The following two theorems are used to derive the energy pumping formula (Eq. (6)) of the main text. Particularly, Theorem 4 relates the derivative  $\partial_{\mu} \mathcal{A}_t$  to the non-abelian Berry curvature tensor  $\mathcal{F}_{t\mu}$ .

**Theorem 3.** *Let us construct a generic projector  $\Pi_{\varphi} = \sum_{m \in S} \Pi_{\varphi}^m$  as a partial sum of indices over a set  $S$ . Then*

$$\partial_{\mu} \Pi_{\varphi} = -i[\mathcal{A}_{\mu}(\varphi), \Pi_{\varphi}]. \quad (29)$$

*Proof.* Let us compute the right hand side of the above equation

$$\begin{aligned} -i[\mathcal{A}_{\mu}, \Pi_{\varphi}] &= \frac{1}{2} \sum_n \sum_{m \in S} [[\partial_{\mu} \Pi_{\varphi}^n, \Pi_{\varphi}^n], \Pi_{\varphi}^m] \\ &= \frac{1}{2} \sum_n \sum_{m \in S} ((\partial_{\mu} \Pi_{\varphi}^n) \Pi_{\varphi}^n \Pi_{\varphi}^m - \Pi_{\varphi}^n (\partial_{\mu} \Pi_{\varphi}^n) \Pi_{\varphi}^m - \Pi_{\varphi}^m (\partial_{\mu} \Pi_{\varphi}^n) \Pi_{\varphi}^n + \Pi_{\varphi}^m \Pi_{\varphi}^n (\partial_{\mu} \Pi_{\varphi}^n)) \\ &= \frac{1}{2} \sum_{m \in S} [(\partial_{\mu} \Pi_{\varphi}^m) \Pi_{\varphi}^m + \Pi_{\varphi}^m (\partial_{\mu} \Pi_{\varphi}^m)] - \frac{1}{2} \sum_{m \in S} \sum_{n \neq m} [\Pi_{\varphi}^n (\partial_{\mu} \Pi_{\varphi}^m) \Pi_{\varphi}^m + \Pi_{\varphi}^m (\partial_{\mu} \Pi_{\varphi}^n) \Pi_{\varphi}^n] \\ &= \frac{1}{2} \partial_{\mu} \Pi_{\varphi} + \frac{1}{2} \sum_{m \in S} \sum_{n \neq m} [\Pi_{\varphi}^n (\partial_{\mu} \Pi_{\varphi}^m) + (\partial_{\mu} \Pi_{\varphi}^m) \Pi_{\varphi}^n] \\ &= \frac{1}{2} \partial_{\mu} \Pi_{\varphi} + \frac{1}{2} \sum_{m \in S} [(1 - \Pi_{\varphi}^m) (\partial_{\mu} \Pi_{\varphi}^m) + (\partial_{\mu} \Pi_{\varphi}^m) (1 - \Pi_{\varphi}^m)] \\ &= \partial_{\mu} \Pi_{\varphi}. \end{aligned} \quad (30)$$

Note that in the third line, we have used the property that  $\Pi_{\varphi}^n (\partial_{\mu} \Pi_{\varphi}^n) \Pi_{\varphi}^n = 0$ .  $\square$

**Theorem 4.** *Define the subspace projected Kato potential*

$$\mathcal{A}_{\mu}^{(\Pi)}(\varphi) = \Pi_{\varphi} \mathcal{A}_{\mu}(\varphi) \Pi_{\varphi}. \quad (31)$$

*Then*

$$\Pi_{\varphi} (\partial_{\mu} \mathcal{A}_{\nu}(\varphi)) \Pi_{\varphi} = \Pi_{\varphi} (\partial_{\mu} \mathcal{A}_{\nu}^{(\Pi)}(\varphi)) \Pi_{\varphi} - \mathcal{F}_{\mu\nu}^{(\Pi)}(\varphi) \quad (32)$$

*where the last term is the non-abelian Berry curvature defined on this subspace*

$$\mathcal{F}_{\mu\nu}^{(\Pi)}(\varphi) = i \Pi_{\varphi} [\partial_{\mu} \Pi_{\varphi}, \partial_{\nu} \Pi_{\varphi}] \Pi_{\varphi}. \quad (33)$$

*Proof.* Let us compute the projected derivative of the Kato gauge potential (we drop the notation of explicit  $\varphi$ -dependence in the following for simplicity)

$$\begin{aligned} \Pi (\partial_{\mu} \mathcal{A}_{\nu}) \Pi &= \partial_{\mu} (\Pi \mathcal{A}_{\nu} \Pi) - (\partial_{\mu} \Pi) \mathcal{A}_{\nu} \Pi - \Pi \mathcal{A}_{\nu} (\partial_{\mu} \Pi) \\ &= \partial_{\mu} \mathcal{A}_{\nu}^{(\Pi)} + i[\mathcal{A}_{\mu}, \Pi] \mathcal{A}_{\nu} \Pi + i \Pi \mathcal{A}_{\nu} [\mathcal{A}_{\mu}, \Pi] \\ &= \partial_{\mu} \mathcal{A}_{\nu}^{(\Pi)} + i \mathcal{A}_{\mu} \Pi \mathcal{A}_{\nu} \Pi - i \Pi \mathcal{A}_{\mu} \mathcal{A}_{\nu} \Pi + i \Pi \mathcal{A}_{\nu} \mathcal{A}_{\mu} \Pi - i \Pi \mathcal{A}_{\nu} \Pi \mathcal{A}_{\mu}. \end{aligned}$$

Applying projector  $\Pi$  on from left and right on both sides of the above equation, we obtain

$$\Pi(\partial_\mu \mathcal{A}_\nu)\Pi = \Pi(\partial_\mu \mathcal{A}_\nu^{(\Pi)})\Pi - i[\Pi \mathcal{A}_\mu(1 - \Pi)\mathcal{A}_\nu \Pi - \Pi \mathcal{A}_\nu(1 - \Pi)\mathcal{A}_\mu \Pi] \quad (34)$$

From the non-abelian Berry curvature defined in terms of the projector in Eq. (33), and using Theorem 3, we obtain

$$\begin{aligned} \mathcal{F}_{\mu\nu}^{(\Pi)} &= i\Pi[\partial_\mu \Pi, \partial_\nu \Pi]\Pi = -i\Pi[[\mathcal{A}_\mu, \Pi], [\mathcal{A}_\nu, \Pi]]\Pi \\ &= -i\Pi[\mathcal{A}_\mu \Pi \mathcal{A}_\nu \Pi - \Pi \mathcal{A}_\mu \mathcal{A}_\nu \Pi - \mathcal{A}_\mu \Pi \Pi \mathcal{A}_\nu + \Pi \mathcal{A}_\mu \Pi \mathcal{A}_\nu]\Pi - (\mu \leftrightarrow \nu) \\ &= -i(\Pi \mathcal{A}_\mu \Pi \mathcal{A}_\nu \Pi - \Pi \mathcal{A}_\mu \mathcal{A}_\nu \Pi) - (\mu \leftrightarrow \nu) \\ &= i\Pi \mathcal{A}_\mu(1 - \Pi) \mathcal{A}_\nu \Pi - i\Pi \mathcal{A}_\nu(1 - \Pi) \mathcal{A}_\mu \Pi, \end{aligned} \quad (35)$$

which is exactly the second term in Eq. (34). Note that  $\Pi \mathcal{F}_{\mu\nu}^{(\Pi)} \Pi = \mathcal{F}_{\mu\nu}^{(\Pi)}$ .  $\square$

In the last theorem, we show that the non-abelian Berry curvature defined in terms of the projectors in Eq. (33) coincide with definition of Wilczek and Zee [39].

**Theorem 5.** *Let  $\{|\alpha\rangle\}$  be a basis of a subspace with projector  $\Pi$ , namely  $\Pi = \sum_\alpha |\alpha\rangle\langle\alpha|$ . Let us denote the matrix elements  $F_{\mu\nu}^{\alpha\beta} \equiv \langle\alpha| \mathcal{F}_{\mu\nu}^{(\Pi)} |\beta\rangle$ . Then this matrix  $F_{\mu\nu}$  can be computed from*

$$F_{\mu\nu} = \partial_\mu A_\nu - \partial_\nu A_\mu - i[A_\mu, A_\nu], \quad (36)$$

where  $A_\mu$  is the non-abelian Wilczek-Zee connection, generalizing abelian Berry connection, defined as  $A_\mu^{\alpha\beta} = \langle\alpha| i\partial_\mu |\beta\rangle$ .

*Proof.* Using the definition of the non-abelian Berry curvature, we have

$$F_{\mu\nu}^{\alpha\beta} = i\langle\alpha| [\partial_\mu \Pi, \partial_\nu \Pi] |\beta\rangle \quad (37)$$

$$= i\langle\partial_\mu \alpha| (1 - \Pi) |\partial_\nu \beta\rangle - (\mu \leftrightarrow \nu) \quad (38)$$

$$= \left[ i\langle\partial_\mu \alpha| \partial_\nu \beta\rangle - i \sum_\gamma \langle\partial_\mu \alpha| \gamma\rangle \langle\gamma| \partial_\nu \beta\rangle \right] - (\mu \leftrightarrow \nu) \quad (39)$$

$$= \partial_\mu A_\nu^{(\alpha\beta)} - \partial_\nu A_\mu^{(\alpha\beta)} - i \sum_\gamma [A_\mu^{\alpha\gamma} A_\nu^{\gamma\beta} - A_\nu^{\alpha\gamma} A_\mu^{\gamma\beta}] \quad (40)$$

$\square$

## DERIVATION OF THE ENERGY PUMPING FORMULA

The energy pumped into drive  $\mu$  can be computed via

$$E_\mu(\varphi_t) = \int_0^t ds \dot{\varphi}_s^\mu \langle\psi(s)| \partial_\mu \mathcal{A}_t(\varphi_s) |\psi(s)\rangle. \quad (41)$$

Since  $|\psi(s)\rangle = \Pi_{\varphi_s}^n |\psi(s)\rangle$ , we have

$$\langle\psi(s)| \partial_\mu \mathcal{A}_t(\varphi_s) |\psi(s)\rangle = \langle\psi(s)| \Pi_{\varphi_s}^n \partial_\mu \mathcal{A}_t(\varphi_s) \Pi_{\varphi_s}^n |\psi(s)\rangle. \quad (42)$$

Using Theorems 1 and 4, we have

$$\Pi_{\varphi_s}^n \partial_\mu \mathcal{A}_t(\varphi_s) \Pi_{\varphi_s}^n = -\mathcal{F}_{\mu t}^n = \mathcal{F}_{t\mu} = \sum_\nu \dot{\varphi}_t^\nu \mathcal{F}_{\nu\mu}^n. \quad (43)$$

Noting that  $\mathcal{F}_{\mu\mu}^n = 0$ , we arrive at the energy pumping formula of the main text

$$E_\mu(\varphi_t) = \int_0^t ds \dot{\varphi}_s^\nu \dot{\varphi}_s^\mu \langle\psi(s)| \mathcal{F}_{\nu\mu}^n(\varphi_s) |\psi(s)\rangle. \quad (44)$$

### DERIVATION OF THE KGP IN THE TRIPOD SYSTEM

The dark state projector  $\Pi = 1 - P$ , where  $P = |\tilde{g}\rangle\langle\tilde{g}|$ , with

$$|\tilde{g}\rangle = \sum_j \Omega_j |g_j\rangle / \Omega, \quad \Omega = \sqrt{\sum_i \Omega_i^2} \quad (45)$$

The KGP can be computed as

$$\begin{aligned} \mathcal{A}_t &= \frac{i}{2} \{ [\partial_t P, P] + [\partial_t (1 - P), (1 - P)] \} \\ &= i(\dot{P}P - P\dot{P}) \\ &= \frac{i}{\Omega^2} \sum_{jk} (\dot{\Omega}_j \Omega_k + \Omega_j \dot{\Omega}_k) [|g_j\rangle\langle g_k| P - P |g_j\rangle\langle g_k|] \\ &= \frac{i}{\Omega^4} \sum_{jkl} \left( \dot{\Omega}_j \Omega_k^2 \Omega_l |g_j\rangle\langle g_l| - \Omega_l \Omega_j^2 \dot{\Omega}_k |g_l\rangle\langle g_k| \right) \\ &= \frac{i}{\Omega^2} \sum_{jk} (\dot{\Omega}_j \Omega_k - \dot{\Omega}_k \Omega_j) |g_j\rangle\langle g_k|. \end{aligned} \quad (46)$$

---